Mon. Not. R. Astron. Soc. **000**, 000–000 (0000) Printed 30 December 2014 (MN LATEX style file v2.2)

Constraints on changes in the proton-electron mass ratio using methanol lines

N. Kanekar[1⋆] W. Ubachs[2], K. M. Menten[3], J. Bagdonaite[3], A. Brunthaler[3], C. Henkel[3,4], S. Muller[5], H. L. Bethlem[2], M. Daprà[2]

[1]*National Centre for Radio Astrophysics, TIFR, Ganeshkhind, Pune - 411007, India*
[2]*Department of Physics and Astronomy, VU University Amsterdam, De Boelelaan 1081, 1081 HV Amsterdam, The Netherlands*
[3]*Max-Planck-Institut für Radioastronomie, Auf dem Hügel 69, 53121, Bonn, Germany*
[4]*Astronomy Department, King Abdulaziz University, PO Box 80203, 21589, Jeddah, Saudi Arabia*
[5]*Department of Earth and Space Sciences, Chalmers University of Technology, Onsala Space Observatory, SE-43992 Onsala, Sweden*

30 December 2014

arXiv:1412.7757v1 [astro-ph.CO] 24 Dec 2014

ABSTRACT

We report Karl G. Jansky Very Large Array (VLA) absorption spectroscopy in four methanol (CH_3OH) lines in the $z = 0.88582$ gravitational lens towards PKS1830−211. Three of the four lines have very different sensitivity coefficients K_μ to changes in the proton-electron mass ratio μ; a comparison between the line redshifts thus allows us to test for temporal evolution in μ. We obtain a stringent statistical constraint on changes in μ by comparing the redshifted 12.179 GHz and 60.531 GHz lines, $[\Delta\mu/\mu] \leqslant 1.1 \times 10^{-7}$ (2σ) over $0 < z \leqslant 0.88582$, a factor of ≈ 2.5 more sensitive than the best earlier results. However, the higher signal-to-noise ratio (by a factor of ≈ 2) of the VLA spectrum in the 12.179 GHz transition also indicates that this line has a different shape from that of the other three CH_3OH lines (at $> 4\sigma$ significance). The sensitivity of the above result, and that of all earlier CH_3OH studies, is thus likely to be limited by unknown systematic errors, probably arising due to the frequency-dependent structure of PKS1830−211. A robust result is obtained by combining the three lines at similar frequencies, 48.372, 48.377 and 60.531 GHz, whose line profiles are found to be in good agreement. This yields the 2σ constraint $[\Delta\mu/\mu] \lesssim 4 \times 10^{-7}$, the most stringent current constraint on changes in μ. We thus find no evidence for changes in the proton-electron mass ratio over a lookback time of ≈ 7.5 Gyrs.

Key words: atomic processes — galaxies: high-redshift — quasars: absorption lines — radio lines: galaxies — galaxies: individual (PKS1830−211)

1 INTRODUCTION

Astronomical spectroscopy in redshifted spectral lines has long been known to provide a probe of changes in the fundamental constants of physics (e.g. the fine structure constant α, the proton-electron mass ratio $\mu \equiv m_p/m_e$, etc.), over large fractions of the age of the Universe (e.g. Savedoff 1956). Such temporal evolution is a generic prediction of field theories that attempt to unify the Standard Model of particle physics and general relativity (e.g. Marciano 1984; Damour & Polyakov 1994). The exciting possibility of low-energy tests of such unification theories has inspired a number of methods to probe fundamental constant evolution on a range of timescales, (see, e.g., Uzan 2011, for a recent review). Most of these methods, both in the laboratory and at cosmological distances, have been sensitive to changes in the fine structure constant α (e.g. Webb et al. 2001; Peik et al. 2004; Gould et al. 2006; Rosenband et al. 2008; Molaro et al. 2013). However, fractional changes in μ are expected to be far larger than those in α in most theoretical scenarios, by factors of $10-500$ (e.g. Calmet & Fritzsch 2002; Langacker et al. 2002).

For many years, ultraviolet ro-vibrational molecular hydrogen (H_2) lines provided the only technique to probe changes in μ on Gyr timescales (Thompson 1975; Varshalovich & Levshakov 1993; Ubachs et al. 2007). The resulting sensitivity to $[\Delta\mu/\mu]$ has been limited by the paucity of redshifted H_2 absorbers (e.g. Noterdaeme et al. 2008), systematic effects in the wavelength calibration of optical spectrographs (Griest et al. 2010; Whitmore et al. 2010; Molaro et al. 2013; Rahmani et al. 2013), and the low sensitivity of H_2 lines to changes in μ. The best limits on fractional changes in μ from this technique are $[\Delta\mu/\mu] \lesssim 10^{-5}$ (2σ) at redshifts $0 < z \lesssim 3$ (e.g. King et al. 2011; van Weerdenburg et al. 2011; Rahmani et al. 2013; Bagdonaite et al. 2014; Albornoz Vásquez et al. 2014).

The situation has changed dramatically in recent years with the development of new techniques using redshifted radio lines from different molecular species (e.g. Darling

⋆ E-mail: nkanekar@ncra.tifr.res.in; Swarnajayanti Fellow

© 0000 RAS

2003; Chengalur & Kanekar 2003; Flambaum & Kozlov 2007; Jansen et al. 2011; Levshakov et al. 2011). While the number of cosmologically-distant radio molecular absorbers is even smaller than the number of high-z H_2 absorbers (just 5 radio systems; Wiklind & Combes 1994; Wiklind & Combes 1995, 1996a,b; Kanekar et al. 2005), the high sensitivity of tunneling transition frequencies in ammonia (NH_3; van Veldhoven et al. 2004; Flambaum & Kozlov 2007) and methanol (CH_3OH; Jansen et al. 2011; Levshakov et al. 2011) to changes in μ has resulted in our best present constraints on changes in any fundamental constant on cosmological timescales. For example, Kanekar (2011) obtained $[\Delta\mu/\mu] < 2.4 \times 10^{-7}$ (2σ) from a comparison between the redshifts of CS, H_2CO and NH_3 lines from the $z \approx 0.685$ system towards B0218+357, while Bagdonaite et al. (2013) obtained $[\Delta\mu/\mu] \leqslant 2.6 \times 10^{-7}$ (2σ) using CH_3OH lines at $z \approx 0.88582$ towards PKS1830−211.

The best techniques to probe fundamental constant evolution are those that use spectral lines from a *single species*, of similar excitation and frequency (e.g. H_2, OH, FeII, CH_3OH; Thompson 1975; Darling 2003; Chengalur & Kanekar 2003; Kanekar & Chengalur 2004; Kanekar et al. 2004; Quast et al. 2004; Jansen et al. 2011). The different lines are then likely to arise in the same gas, implying that local velocity offsets should not be a source of systematic effects. The CH_3OH technique is especially interesting because CH_3OH has many strong radio lines with different frequency dependences on μ; different line combinations thus provide independent probes of any evolution (Jansen et al. 2011; Levshakov et al. 2011). In this *Letter*, we report a robust new constraint on changes in μ from CH_3OH spectroscopy of the $z = 0.88582$ gravitational lens towards PKS1830−211 with the Karl G. Jansky Very Large Array (VLA).

2 OBSERVATIONS, DATA ANALYSIS AND SPECTRA

The VLA observations of the methanol lines at $z = 0.88582$ towards PKS1830−211 were carried out in 2012 July and August, in the B-configuration (proposal 12A-389). Four CH_3OH lines were targeted, the $2_0 - 3_{-1}$ E, $1_0 - 0_0$ A^+ and E, and 1_0-2_{-1} E transitions at $12.178597(4)$ GHz, $48.3724558(7)$ GHz, $48.376892(10)$ GHz, and $60.531489(10)$ GHz, respectively (for the line frequencies, see Müller et al. 2004, and references therein). These are redshifted to observing frequencies of ≈ 6.46 GHz (C-band), 25.65 GHz (two lines; K-band) and 32.10 GHz (Ka-band), respectively. The VLA C-band observations covering the redshifted 12.179 GHz line were carried out on July 13 and 14 (total on-source time: 7 hours), with both the K- and Ka-band observations on August 12, with on-source times of 1.5 hours (Ka-band) and 0.5 hours (K-band, covering both redshifted 48 GHz lines).

We note, in passing, that the 12.179 GHz line has the largest sensitivity coefficient ($K_\mu \approx -32$) to changes in μ, but is also the weakest of the CH_3OH lines that has been detected in the $z = 0.88582$ absorber (Bagdonaite et al. 2013). All earlier studies using the CH_3OH lines to probe changes in μ have been limited by the low signal-to-noise ratio in this transition (e.g. Bagdonaite et al. 2013,?). We hence chose to obtain a deep spectrum in this line, spending the maximum integration time on its observations.

Bandwidths of 8 MHz (C-band) and 32 MHz (K- and Ka-bands) were used in each of two intermediate frequency (IF) bands, which were further sub-divided into eight digital sub-bands, each with 128 channels. The two IF bands were offset from each other by half a digital sub-band, to ensure uniform sensitivity across the final spectra. Observations of 3C286, J1733−1304 (K- and Ka-bands) and J1229+0203 (C-band) were used to calibrate the flux density scale and the antenna bandpasses. No phase calibrator was observed, as PKS1830−211 is bright enough for self-calibration. Online Doppler tracking was not used.

All data were analysed in "classic" AIPS, following standard procedures. For each band, after initial data editing, and flux and bandpass calibration, a number of absorption-free PKS1830−211 channels were averaged to form a "channel-0" dataset. A standard self-calibration procedure was then used to determine the antenna-based gains, until the gains and the image converged. The tasks UVSUB and UVLIN were used to subtract PKS1830−211's continuum from the calibrated visibilities, and CVEL then used to shift the residual visibilities to the heliocentric frame. Each dataset was imaged to produce a spectral cube, with natural weighting used to maximise the sensitivity. This yielded cubes with angular resolutions of $\approx 0.4'' \times 0.2''$ (Ka-band), $0.66'' \times 0.34''$ (K-band) and $2.1'' \times 1.1''$ (C-band); the two components of PKS1830−211 (separated by $\approx 1''$; Rao & Subrahmanyan 1988) were thus marginally resolved at K- and Ka-band. Finally, the CH_3OH spectra were obtained via a cut through the location of the S-W source component against which the strong molecular absorption is seen (e.g. Frye et al. 1997; Muller et al. 2006). At each frequency, the spectra from the two IF bands were combined to obtain the final spectrum. The C-band spectra from the two runs were combined using weights based on their root-mean-square (RMS) noise values.

The final VLA CH_3OH optical depth spectra are shown in Fig. 1. The optical depth RMS noise values against the S-W source component are 0.0062 per 0.58 km s^{-1} (Ka-band), 0.0048 per 0.73 km s^{-1} (K-band), and 0.00041 per 0.73 km s^{-1} (C-band). These optical depth estimates assume that 40% of the flux density of PKS1830−211 is in the S-W component. For comparison, the Effelsberg spectra of Bagdonaite et al. (2013,?) had optical depth RMS noise values of 0.0033 per 1.8 km s^{-1} (Ka-band), 0.0013 per 2.3 km s^{-1} (K-band) and 0.00040 per 2.3 km s^{-1} (C-band). As noted earlier, the best current analyses (Bagdonaite et al. 2013,?) have been limited by the sensitivity in the redshifted 12.179 GHz transition. The sensitivity of the VLA C-band spectrum in this transition is a factor of ≈ 1.8 better than that of the best earlier spectra.

3 PROBING FUNDAMENTAL CONSTANT EVOLUTION

A critical question in using multiple spectral lines to probe fundamental constant evolution is whether or not the lines arise in the same gas. This is important because any measured differences in the line redshifts might arise due to local velocity offsets in the absorbing gas. Unfortunately, it is not guaranteed that different transitions arise in the same gas, even for absorption lines from the same species, especially for gravitational lenses like the $z = 0.88582$ system towards PKS1830−211. For example, time variability in the structure of the background source could cause differences in the paths traced by different transitions, if the lines are not observed simultaneously (e.g. Muller & Guélin 2008). Conversely, frequency-dependent structure in the background source could cause absorption at different frequencies (even if observed simultaneously) to probe different sightlines through the absorbing gas (e.g. Martí-Vidal et al. 2013; Bagdonaite et al. 2013). In the case of PKS1830−211, the S-W source component is known to be scatter-broadened, and hence more extended, at low frequencies (e.g. Jones et al. 1996), due to which the C-band and K-/Ka-band observations may trace slightly different gas.

Transition	Rest frequency GHz	K_μ	Redshift	FWHM km s^{-1}	Peak optical depth
$2_{-1} - 1_0$ E	60.531489(10)	−7.4	0.8858052(19)		0.0433(15)
$0_0 - 1_0$ A$^+$	48.3724558(7)	−1.0	0.8858010(14)	13.85(0.39)	0.0566(18)
$0_0 - 1_0$ E	48.376892(10)	−1.0	0.8858010(14)		0.01893(66)

Table 1. Parameters of the best single-component Gaussian fit to the 60.531 GHz, 48.372 GHz, and 48.377 GHz lines. The second and third columns give the line rest frequencies (as measured in the laboratory; Heuvel & Dymanus 1973; Breckenridge & Kukolich 1995; Müller et al. 2004) and the sensitivity coefficents to changes in μ (Jansen et al. 2011). The redshifts of the 48.372 and 48.377 GHz lines were tied together in the fit (as these transitions have the same K_μ value), as were the column densities in the 60.531 and 48.377 GHz lines (both E-type transitions). All three line FWHMs were also assumed to be the same. The measured redshifts, listed in column (4), are in the heliocentric frame.

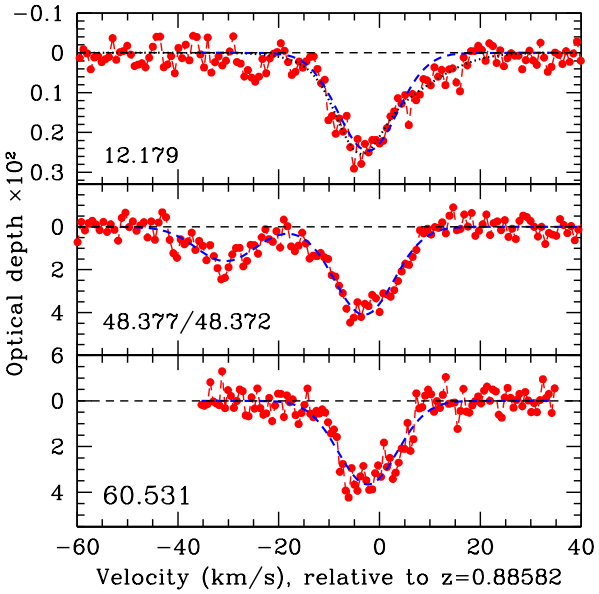

Figure 1. VLA CH_3OH spectra at $z = 0.88582$ towards PKS1830−211, with optical depth against the S-W image plotted against velocity, relative to $z = 0.88582$ (heliocentric). The three panels show the 60.531 GHz line (bottom), the 48.372 and 48.377 GHz lines (middle), and the 12.179 GHz line (top); the velocity scale in the middle panel is for the 48.372 GHz line. The dashed curves in the lower two panels indicate the best-fit 1-Gaussian model that was obtained from a simultaneous fit to the 60.531, 48.372 and 48.377 GHz lines, with the line FWHMs tied together. The dashed curve in the top panel shows the above (scaled) 1-Gaussian model overlaid on the spectrum in the 12.179 GHz transition; this model does not appear to provide a good fit to the weak absorption wing that extends beyond ≈ 10 km s^{-1}. The dotted curve in the top panel shows a 2-Gaussian model that gives a good fit to the spectrum in the 12.179 GHz line.

A basic test of whether different lines arise in the same gas is whether or not they have the same velocity structure. This can be simply tested by fitting the same template to the line profiles and checking whether the fit parameters (except for the amplitude) are in agreement. A multi-Gaussian template profile was used for this purpose, with independent fits to the redshifted 12.179 GHz and 60.531 GHz lines, and a joint fit to the redshifted 48.372 GHz and 48.377 GHz lines (which are blended). The 60.531 GHz, 48.372 GHz and 48.377 GHz lines were all found to be well fit by a single Gaussian component (with reduced chi-square values $\chi^2_\nu \approx 1$), with the line full widths at half maximum (FWHMs) in good agreement (within 2σ significance). However, the single Gaussian fit to the 12.179 GHz line yielded a line FWHM that was larger than the FWHM of the other lines, at 4.3σ significance. Further, this fit yielded $\chi^2_\nu = 1.3$, with statistically significant residuals, suggesting that additional components are needed to model the line. This is also visually apparent from Fig. 1, where the 12.179 GHz line extends to ≈ 18 km s^{-1}, unlike the 60.531 GHz and 48.372 GHz lines. Thus, the 60.531 GHz, 48.372 GHz and 48.377 GHz lines appear likely to arise from the same sightline (as their line FWHMs are in agreement), while the sightline of the 12.179 GHz transition is likely to be different.

The most likely cause of this difference in sightlines is the frequency-dependent structure of PKS1830−211[1], due to the larger scatter-broadening of the S-W source component at low frequencies (e.g. Jones et al. 1996). This would account for the larger velocity spread in the lower-frequency C-band transition, as this sightline would intersect a larger transverse region through the absorber, and hence, a more extended velocity field. Note that the size of the S-W radio emission changes dramatically with frequency, from > 50 mas at 2.3 GHz to < 10 mas at 8.4 GHz, with 6.46 GHz, the redshifted 12.179 GHz line frequency, in between (Guirado et al. 1999). The size diminishes even further at higher frequencies: at 14.5, 23.2 and 43 GHz, almost all the S-W emission is concentrated in a compact source with FWHM < 0.5 mas, representing the image of the AGN core without scatter broadening (Jin et al. 2003; Sato et al. 2013). At $z = 0.88582$, 1 mas corresponds to 8 pc, implying that we are probing scales of $\sim$ 100 pc (i.e. the size of a typical Giant Molecular Cloud, GMC) at 6.46 GHz, but only $\sim$ 5 pc (i.e. a small part of a GMC) at 32.10 GHz. This makes velocity differences of a few km s^{-1} and different line shapes certainly plausible. The above issue was considered by Bagdonaite et al. (2013), who assumed that it could cause a shift of $\approx$ 1 km s^{-1} between the different lines (Martí-Vidal et al. 2013); unfortunately, it is difficult to directly estimate the systematic error here. It thus appears that the 12.179 GHz line should not be compared with the higher-frequency CH_3OH lines to probe changes in μ. The other three lines, closer in frequency, are likely to arise from the same gas and hence appear to be well-suited for use in probing fundamental constant evolution. However, since the difference in line FWHMs has only $\approx 4.3\sigma$

[1] The 1-month separation between the C-band and K-/Ka-band observations may also contribute to the differences, especially given that there was a gamma-ray flare in PKS1830−211 in May–July 2013 (Martí-Vidal et al. 2013).

significance, we provide below results based on both analyses, i.e. both including and excluding the 12.179 GHz line.

We used two independent approaches to test for changes in the proton-electron mass ratio: (1) a joint multi-Gaussian fit to the 60.531 GHz, 48.372 GHz and 48.377 GHz lines, and (2) cross-correlation of individual pairs of lines. The advantage of the former is that it implicitly tests whether all the lines can be fit with the same template (i.e. the same number of Gaussian components, with the same FWHMs). Furthermore, the joint fit simultaneously makes use of all the information in the different lines (e.g. Webb et al. 2001; Molaro et al. 2013; Rahmani et al. 2013). Conversely, the advantage of the cross-correlation approach is that it is non-parametric, making no assumptions about the line shapes or the number of components that must be fit to the lines (which can affect the results, especially for complex line profiles) (e.g. Kanekar et al. 2004, 2010; Levshakov et al. 2012).

In the first approach, the package VPFIT was used to carry out a simultaneous multi-Gaussian fit to the 60.531 GHz, 48.372 GHz and 48.377 GHz lines, aiming to minimize χ^2_ν by varying the fit parameters[2] . The velocity structure was assumed to be the same in all the lines, with the same number of components and the same velocity widths (which were hence assumed to be the same in the fitting process). This essentially assumes that all the lines arise in the same absorbing gas. Since the 48.372 GHz and 48.377 GHz lines have the same sensitivity coefficient to changes in μ ($K_\mu = -1$), these line redshifts were also assumed to be the same. Finally, the 60.531 GHz and 48.377 GHz lines are both E-type lines (the 48.372 GHz line is an A-type); local thermal equilibrium was assumed for the ratios of the strengths of the E-type lines.

A single component Gaussian model was found to yield an excellent fit to all three lines, with $\chi^2_\nu = 1.07$, and noise-like residuals (via a Kolmogorov-Smirnov rank-1 test) in each spectrum, after subtracting out the fitted profiles. Five free parameters (listed in Table 1) were used in the fit, two column densities for the E-type and A-type lines (see above), a single FWHM for all lines, and two redshifts for the 60.531 GHz line and the pair of 48 GHz lines. The velocity offset between the redshifts of the 60.531 GHz line (z_A) and the 48 GHz pair (z_B) is given by $\Delta V/c = (z_A - z_B)/(1 + \bar{z})$, where $\bar{z}$ is the average of the two redshifts. This yields $\Delta V = (+0.66 \pm 0.39)$ km s^{-1}, i.e. $[\Delta\mu/\mu] = (\Delta V/c) \times (K_{\mu,A} - K_{\mu,B}) = (-3.5 \pm 2.0) \times 10^{-7}$, where $K_{\mu,A} = -7.4$ and $K_{\mu,B} = -1$ are the sensitivity coefficients of the 60.531 GHz line and the 48 GHz pair to changes in μ. Similar results were obtained on removing the assumption that the two 48 GHz lines (A- and E-types) arise at the same redshift.

The second approach was carried out on individual pairs of lines using two non-parametric schemes, the cross-correlation method (Kanekar et al. 2004) and the "sliding-distance" method (Levshakov et al. 2012). These yielded very similar results, so we will only discuss the cross-correlation approach in detail. The cross-correlation of the two strongest lines, at 60.531 GHz and 48.372 GHz, yielded a velocity offset of $\Delta V = (+0.46 \pm 0.43)$ km s^{-1}, with the 60.531 GHz line at higher velocities. The RMS error was estimated by cross-correlating 10^4 pairs of simulated spectra, obtained by adding independent representations of Gaussian noise to the best-fit profiles, with the noise spectra characterized by the RMS noise values of the observed spectra. This yields $[\Delta\mu/\mu] = (-2.4 \pm 2.3) \times 10^{-7}$, similar to the result obtained earlier from the Gaussian-fitting analysis. The slightly higher error in the cross-correlation approach is because only the two strongest lines were used here, so all the information available in the joint Gaussian-fitting has not been used. Further, the entire velocity range was not used in the cross-correlation, with the velocity interval containing a blend of the 48.372 GHz and 48.377 GHz lines excluded from the analysis, to reduce systematic errors.

The analysis using the 12.179 GHz line was restricted to the cross-correlation approach. This also takes into account the possibility that the 12.179 GHz line might not be offset in velocity from the other lines, but might merely have additional spectral components, in addition to the strongest component seen in the other lines. A cross-correlation analysis was hence carried out on the 12.179 GHz and 60.531 GHz pair, following the approach detailed above. This yielded a velocity offset of $\Delta V = (+0.22 \pm 0.43)$ km s^{-1}, again with the 60.531 GHz line at higher velocities, giving $[\Delta\mu/\mu] = (-2.9 \pm 5.7) \times 10^{-8}$. Again, no evidence is seen for changes in μ with cosmological time.

4 DISCUSSION AND CONCLUSIONS

The $z = 0.88582$ absorber towards PKS1830−211 is the only object so far with a detection of redshifted CH_3OH absorption (Muller et al. 2011) and has hence been the focus of tests of changes in the proton-electron mass ratio using these lines. Initially, Ellingsen et al. (2012) obtained $[\Delta\mu/\mu] \leqslant 4.2 \times 10^{-7}$ (at 2σ significance), via a comparison between the redshifts of the 12.179 GHz and the 60.531 GHz lines. Later, Bagdonaite et al. (2013) improved this to $[\Delta\mu/\mu] \leqslant 2 \times 10^{-7}$, using the 12.179 GHz, 48.372 GHz, 48.377 GHz and 60.531 GHz lines. Most recently, Bagdonaite et al. (2013) combined the 12.179 GHz line with nine other lines, at rest frequencies $\leqslant 492.279$ GHz, and also carried out a multi-dimensional regression analysis to include systematic effects in their error budget, to obtain $[\Delta\mu/\mu] \leqslant 2.6 \times 10^{-7}$ (2σ) (combining statistical and systematic errors in quadrature). In the present work, we have combined the 12.179 GHz line with the 60.531 GHz line to obtain a constraint of high apparent sensitivity, $[\Delta\mu/\mu] \leqslant 1.1 \times 10^{-7}$ (2σ), a factor of ≈ 2.5 better than the best earlier results (Bagdonaite et al. 2013).

All the earlier analyses used independent fits to the different lines and did not directly test whether the lines arise in the same gas. The 12.179 GHz line was a critical component of all analyses, especially because this line has $K_\mu = -32$, one of the largest sensitivity coefficients of the CH_3OH lines. Including this line in the comparison thus gives a large lever arm (i.e. a large ΔK_μ) in tests of changes in μ. Unfortunately, this is one of the weaker CH_3OH lines, and its spectra have had the lowest signal-to-noise ratios of the lines that have been used so far. As noted earlier (Bagdonaite et al. 2013), this is also the line that is most likely to be affected by differing sightlines, due to the large scatter broadening of the S-W source component of PKS1830−211 at the low line frequency. The relatively low sensitivity of the earlier spectra in this transition has meant that it has not been possible to test whether the line shape is the same as that of the other CH_3OH lines.

Our new, higher-sensitivity, VLA spectrum indicates that the 12.179 GHz line profile is indeed different from the other three line profiles: the line FWHM is larger, at $\approx 4.3\sigma$ significance, and the 1-Gaussian model yields a relatively high reduced chi-square value, $\chi^2_\nu \approx 1.3$. This suggests that the sightline in the 12.179 GHz

[2] Note that little is known about the CH_3OH hyperfine structure which has been ignored here. For a few lines, Heuvel & Dymanus (1973) find the hyperfine structure extends over $\lesssim 50$ kHz, i.e. smaller than our channel spacing; it should have a negligible effect on our results.

transition traces different absorbing gas from that detected in the other three lines. If so, this implies that analyses that include the 12.179 GHz transition (i.e. all earlier results from the $z = 0.88582$ absorber, as well as our result above) would incur unknown systematic errors due to local velocity structure in the gas.

We hence recommend that the 12.179 GHz line should not be used with the high-frequency CH_3OH lines from the $z = 0.88582$ absorber to probe changes in the proton-electron mass ratio. The best probe of changes in μ using the CH_3OH lines is likely to arise from a combination of the 48.372/48.377 GHz pair and the 60.531 GHz line, since these lines both have a large difference between sensitivity coefficients ($\Delta K_\mu = 6.4$), and lie at nearby observing frequencies, where the background source has a similar structure (S-W component size < 0.5 mas; Jin et al. 2003; Sato et al. 2013). The lines should be observed simultaneously, so that time variability in PKS1830−211 does not cause systematic errors. Finally, our current result from these lines, $[\Delta\mu/\mu] \lesssim 4 \times 10^{-7}$ (2σ), is based on a fairly short VLA integration time (2 hrs). Deeper VLA spectroscopy in these lines will allow a significant improvement in the sensitivity to temporal changes in μ.

In conclusion, our VLA observations of the CH_3OH lines from the $z = 0.88582$ absorber towards PKS1830−211 suggest that the shape of the 12.179 GHz line is different from that of the 48.372, 48.377 and 60.531 GHz lines. The FWHM of the 12.179 GHz line is different from that of the other lines at $\approx 4.3\sigma$ significance, and the best fit with a 1-Gaussian model has a relatively high reduced chi-square value, $\chi^2_\nu \approx 1.3$, in contrast to similar fits to the other three lines, which yield $\chi^2_\nu \approx 1$. Including the 12.179 GHz line in the analysis to probe changes in μ gives a high statistical sensitivity to changes in μ: $[\Delta\mu/\mu] = (-2.9 \pm 5.7) \times 10^{-8}$, i.e. $[\Delta\mu/\mu] \leqslant 1.1 \times 10^{-7}$ at 2σ significance. While this constraint on changes in μ is a factor of ≈ 2.5 better than the best earlier results using CH_3OH lines, both it and all earlier CH_3OH analyses in the literature appear likely to be subject to unknown systematic errors due to the difference in the shapes of the 12.179 GHz line and the higher-frequency CH_3OH lines. The CH_3OH 48.372, 48.377 and 60.531 GHz lines have shapes consistent with each other and are thus likely to arise in the same gas. Our most robust result, obtained via both joint Gaussian-fitting and cross-correlation approaches, stems from combining the three high-frequency lines: $[\Delta\mu/\mu] \lesssim 4 \times 10^{-7}$ (2σ). While this gives an apparently less stringent constraint than that from analyses that include the 12.179 GHz line, the fact that the lines used in the analysis have the same shape suggests that it is the most reliable of the present constraints on changes in μ based on CH_3OH spectroscopy. We thus find no evidence for changes in the proton-electron mass ratio out to $z = 0.88582$, with $[\Delta\mu/\mu] \lesssim 4 \times 10^{-7}$ (2σ) over a lookback time of ≈ 7.5 Gyr.

ACKNOWLEDGMENTS

The National Radio Astronomy Observatory is a facility of the National Science Foundation, operated under cooperative agreement by Associated Universities, Inc. NK acknowledges support from the DST, India, via a Swarnajayanti Fellowship.

REFERENCES

Albornoz Vásquez D., Rahmani H., Noterdaeme P., Petitjean P., Srianand R., Ledoux C., 2014, A&A, 562, A88
Bagdonaite J., Daprà M., Jansen P., Bethlem H. L., Ubachs W., Muller S., Henkel C., Menten K. M., 2013, Phys. Rev. Lett., 111, 231101
Bagdonaite J., Jansen P., Henkel C., Bethlem H. L., Menten K. M., Ubachs W., 2013, Science, 339, 46
Bagdonaite J., Ubachs W., Murphy M. T., Whitmore J. B., 2014, ApJ, 782, 10
Breckenridge S. M., Kukolich S. G., 1995, ApJ, 438, 504
Calmet X., Fritzsch H., 2002, Eur. Phys. Jour. C, 24, 639
Chengalur J. N., Kanekar N., 2003, Phys. Rev. Lett., 91, 241302
Damour T., Polyakov A. M., 1994, Nucl. Phys. B, 423, 532
Darling J., 2003, Phys. Rev. Lett., 91, 011301
Ellingsen S. P., Voronkov M. A., Breen S. L., Lovell J. E. J., 2012, ApJ, 747, L7
Flambaum V. V., Kozlov M. G., 2007, Phys. Rev. Lett., 98, 240801
Frye B., Welch W. J., Broadhurst T., 1997, ApJL, 478, L25
Gould C. R., Sharapov E. I., Lamoreaux S. K., 2006, Phys. Rev. C, 74, 024607
Griest K., Whitmore J. B., Wolfe A. M., Prochaska J. X., Howk J. C., Marcy G. W., 2010, ApJ, 708, 158
Guirado J. C., Jones D. L., Lara L., Marcaide J. M., Preston R. A., Rao A. P., Sherwood W. A., 1999, A&A, 346, 392
Heuvel J. E. M., Dymanus A., 1973, Jour. Mol. Spec., 45, 282
Jansen P., Xu L.-H., Kleiner I., Ubachs W., Bethlem H. L., 2011, Phys. Rev. Lett., 106, 100801
Jin C., Garrett M. A., Nair S., Porcas R. W., Patnaik A. R., Nan R., 2003, MNRAS, 340, 1309
Jones D. L. et al., 1996, ApJ, 470, L23
Kanekar N., 2011, ApJ, 728, L12
Kanekar N. et al., 2005, Phys. Rev. Lett., 95, 261301
Kanekar N., Chengalur J. N., 2004, MNRAS, 350, L17
Kanekar N., Chengalur J. N., Ghosh T., 2004, Phys. Rev. Lett., 93, 051302
Kanekar N., Chengalur J. N., Ghosh T., 2010, ApJ, 716, L23
King J. A., Murphy M. T., Ubachs W., Webb J. K., 2011, MNRAS, 417, 301
Langacker P. G., Segré G., Strassler M. J., 2002, Phys. Lett. B, 528, 121
Levshakov S. A., Combes F., Boone F., Agafonova I. I., Reimers D., Kozlov M. G., 2012, A&A, 540, L9
Levshakov S. A., Kozlov M. G., Reimers D., 2011, ApJ, 738, 26
Marciano W. J., 1984, Phys. Rev. Lett., 52, 489
Martí-Vidal I. et al., 2013, A&A, 558, A123
Molaro P. et al., 2013, A&A, 555, A68
Müller H. S. P., Menten K. M., Mäder H., 2004, A&A, 428, 1019
Muller S. et al., 2011, A&A, 535, 103
Muller S., Guélin M., 2008, A&A, 491, 739
Muller S., Guélin M., Dumke M., Lucas R., Combes F., 2006, A&A, 458, 417
Noterdaeme P., Ledoux C., Petitjean P., Srianand R., 2008, A&A, 481, 327
Peik E., Lipphardt B., Schnatz H., Schneider T., Tamm C., Karshenboim S. G., 2004, Phys. Rev. Lett., 93, 170801
Quast R., Reimers D., Levshakov S. A., 2004, A&A, 415, L7
Rahmani H. et al., 2013, MNRAS, 435, 861
Rao A. P., Subrahmanyan R., 1988, MNRAS, 231, 229
Rosenband T. et al., 2008, Science, 319, 1808
Sato M., Reid M. J., Menten K. M., Carilli C. L., 2013, ApJ, 764, 132
Savedoff M. P., 1956, Nature, 178, 688
Thompson R. I., 1975, ApL, 16, 3
Ubachs W., Buning R., Eikema K. S. E., Reinhold E., 2007, J.Mol.Spec., 241, 155
Uzan J.-P., 2011, Living Reviews in Relativity, 14, 2
van Veldhoven J., Küpper J., Bethlem H. L., Sartakov B., van Roij A. J. A., Meijer G., 2004, Eur. Phys. Jour. D, 31, 337
Varshalovich D. A., Levshakov S. A., 1993, JETP, 58, L237
Webb J. K., Murphy M. T., Flambaum V. V., Dzuba V. A., Barrow J. D., Churchill C. W., Prochaska J. X., Wolfe A. M., 2001, Phys. Rev. Lett., 87, 091301
van Weerdenburg F., Murphy M. T., Malec A. L., Kaper L., Ubachs W., 2011, Phys. Rev. Lett., 106, 180802
Whitmore J. B., Murphy M. T., Griest K., 2010, ApJ, 723, 89

Wiklind T., Combes F., 1994, A&A, 286, L9
Wiklind T., Combes F., 1995, A&A, 299, 382
Wiklind T., Combes F., 1996a, A&A, 315, 86
Wiklind T., Combes F., 1996b, Nature, 379, 139